Ultrafast demagnetisation dependence on film thickness: A TDDFT calculation

Cite as: AIP Conference Proceedings **1942**, 130014 (2018); https://doi.org/10.1063/1.5029084
Published Online: 10 April 2018

N. Singh, and S. Sharma

Ultrafast Demagnetisation Dependence On Film Thickness: A TDDFT Calculation

N. Singh[1, 2,a)] and S. Sharma [1]

[1] *Max-Planck-Institut für Mikrostrukturphysik, Weinberg 2, D-06120 Halle, Germany.*
[2] *Department of Physics, Indian Institute of Technology-Roorkee, 247667, Uttarakhand, India.*

[a)] Corresponding author: nsingh@mpi-halle.mpg.de

Abstract. Ferromagnetic materials when subjected to intense laser pulses leads to reduction of their magnetisation on an ultrafast scale. Here, we perform an *ab-initio* calculation to study the behavior of ultrafast demagnetisation as a function of film thickness for Nickel as compared to the bulk of the material. In thin films surface formation results in amplification of demagnetisation with the percentage of demagnetisation depending upon the film thickness.

INTRODUCTION

In 1996, Beaurepaire et.al. introduced Femtomagnetism [1] establishing that the magnetisation can be manipulated on femtosecond timescale by applying intense laser pulses. This triggered several experimental works [2–6] demonstrating laser induced ultrafast demagnetisation in ferromagnets. Such an optical control of spins with light is the holy grail in the field of memory storage.

To understand the underlying physics of femtomagnetism theoretically several studies have been performed and almost all of these are based on simple models [7, 8]. It is only recently a fully *ab-initio* work was performed [9,10] and it concludes that the underlying physics of ultrafast demagnetisation is due to the spin-orbit coupling induced spin-flips [11] in both thin films and bulk. Additionally, in case of the films the symmetry breaking due to the surface formation enhances the demagnetisation [11]. In the present work we further study this physics by varying the thickness of the Nickel films and see that as the film thickness increases the magnitude of demagnetisation decreases.

In order to perform these theoretical calculations we use the Time-Dependent Density Functional Theory (TDDFT) [12–15], which is a well-established and sophisticated *ab-initio* theory to study the light-matter interactions. TDDFT makes no assumptions regarding the underlying physics or the material under investigation and provides us, with a clear picture of laser induced demagnetisation.

Methodology

To capture the demagnetisation process we require a time evolving electronic wave- function, which within TDDFT [14] is obtained from the Kohn-Sham (KS) Hamiltonian given as:

DAE Solid State Physics Symposium 2017
AIP Conf. Proc. 1942, 130014-1–130014-4; https://doi.org/10.1063/1.5029084
Published by AIP Publishing. 978-0-7354-1634-5/$30.00

$$\widehat{\boldsymbol{H}}_S = \left[\frac{1}{2}\left(\widehat{\boldsymbol{p}} + \frac{1}{c}\boldsymbol{A}_{ext}(t)\right)^2 + v_S(\boldsymbol{r},t) + \frac{1}{2c}\boldsymbol{\sigma}.\boldsymbol{B}_S(\boldsymbol{r},t) + \frac{1}{4c^2}\boldsymbol{\sigma}.(\nabla v_S(\boldsymbol{r},t)\times\widehat{\boldsymbol{p}})\right] \quad (1)$$

where c is the speed of light, $\boldsymbol{\sigma}$ are the Pauli matrices and $\boldsymbol{A}_{ext}(\boldsymbol{r},t)$ is the vector potential representing an applied laser field. We disregard the spatial dependence of the vector potential $\boldsymbol{A}_{ext}(\boldsymbol{r},t)$ by considering the so-called dipole approximation. The KS effective potential $v_S(\boldsymbol{r},t) = v_{ext}(\boldsymbol{r},t) + v_H(\boldsymbol{r},t) + v_{XC}(\boldsymbol{r},t)$ comprises of the external potential v_{ext}, the classical electrostatic Hartree potential v_H and the exchange-correlation (XC) potential v_{XC}. Similarly, the KS magnetic field is written as $\boldsymbol{B}_S(\boldsymbol{r},t) = B_{\boldsymbol{ext}}(t) + \boldsymbol{B}_{XC}(\boldsymbol{r},t)$ where $B_{\boldsymbol{ext}}(t)$ corresponds to the magnetic field of the applied laser pulse plus possibly an additional magnetic field and $\boldsymbol{B}_{XC}(\boldsymbol{r},t)$ is the XC magnetic field. For calculating the XC potential and magnetic field the adiabatic local spin density approximation (ALDA) is used. The final term of Eq. (1) is the spin-orbit coupling term.

The dynamics of the magnetisation is given by the Heisenberg equation of motion:

$$\begin{aligned}\frac{\partial}{\partial t}m_i(\boldsymbol{r},t) &= \left\langle\left(\frac{\partial}{\partial t}\psi^\dagger(\boldsymbol{r},t)\right)\widehat{\boldsymbol{\sigma}}_i\psi(\boldsymbol{r},t) + \psi^\dagger(\boldsymbol{r},t)\widehat{\boldsymbol{\sigma}}_i\left(\frac{\partial}{\partial t}\psi(\boldsymbol{r},t)\right)\right\rangle \\ &= i\langle\psi^\dagger(\boldsymbol{r},t)\widehat{\boldsymbol{H}}_S\widehat{\boldsymbol{\sigma}}_i\psi(\boldsymbol{r},t) + \psi^\dagger(\boldsymbol{r},t)\widehat{\boldsymbol{\sigma}}_i(-i)\widehat{\boldsymbol{H}}_S\psi(\boldsymbol{r},t)\rangle \\ &= i\langle[\widehat{\boldsymbol{H}}_S, \widehat{\boldsymbol{\sigma}}_i\hat{n}(\boldsymbol{r},t)]\rangle\end{aligned} \quad (2)$$

where ψ is the two component spinor-valued KS orbital (Pauli spinors) Substituting $\widehat{\boldsymbol{H}}_S$ from Eq. 1 in Eq. 2 and in the absence of external magnetic field (i.e. the materials which are spontaneous magnets) we get

$$\begin{aligned}\frac{\partial}{\partial t}M(t)\Big|_i &= \frac{1}{2c^2}\int d^3r \sum_{j,m}^{3}\epsilon_{ijm}\,\nabla v_s(\boldsymbol{r},t)\times\boldsymbol{J}_m(\boldsymbol{r},t)\Bigg|_j \\ &= \frac{1}{2c^2}\int d^3r \begin{bmatrix}\widehat{\boldsymbol{x}}\\ \widehat{\boldsymbol{y}}\\ \widehat{\boldsymbol{z}}\end{bmatrix}\times\begin{bmatrix}\nabla v_s(\boldsymbol{r},t)\times\boldsymbol{J}_x(\boldsymbol{r},t)\\ \nabla v_s(\boldsymbol{r},t)\times\boldsymbol{J}_y(\boldsymbol{r},t)\\ \nabla v_s(\boldsymbol{r},t)\times\boldsymbol{J}_z(\boldsymbol{r},t)\end{bmatrix}\Bigg|_i\end{aligned} \quad (3)$$

This equation indicates how the dynamics of magnetisation is guided by spin-currents in the system, for example the *z*-component reads:

$$\frac{\partial}{\partial t}M_Z(t) = \frac{1}{2c^2}\int d^3r\ \hat{x}.\left[\nabla v_s(\boldsymbol{r},t)\times\boldsymbol{J}_y(\boldsymbol{r},t)\right] - \hat{y}\,.\left[\nabla v_s(\boldsymbol{r},t)\times\boldsymbol{J}_x(\boldsymbol{r},t)\right] \quad (4)$$

Results

In order to study the behavior of demagnetisation as a function of film thickness we study four cases; laser induced spin dynamics in 3, 5 and 7 atomic layers thick Nickel films and the bulk of Nickel. To study demagnetisation a pump laser pulse is applied perpendicular to the surfaces of the layered Nickel which has the magnetisation pointing in-plane. Application of the laser pulse results in excitation of the electrons to higher energy level which eventually leads to onset of demagnetisation process. We start with the systems at t=0 in their ground state, hit it with a laser pulse of intensity 9.23×109 W/m2 and watch the system evolve in time. The relative magnetic moment M_z (t)/M_z (t = 0) for all the four setups is shown in Fig 1. The percentage of demagnetisation in all the four setups is different being only ~ 15% in bulk. The thin films of Nickel of different thickness show different degree of demagnetisation (~ 40%, ~ 39% and ~ 33% in 3,5 and 7 Monolayers of Nickel respectively) showing the decline in demagnetisation as the thickness of layers increase. The reason of having a higher magnitude of demagnetisation in layers was attributed to a larger spin-current arising on the surface due to the symmetry breaking [9–11].

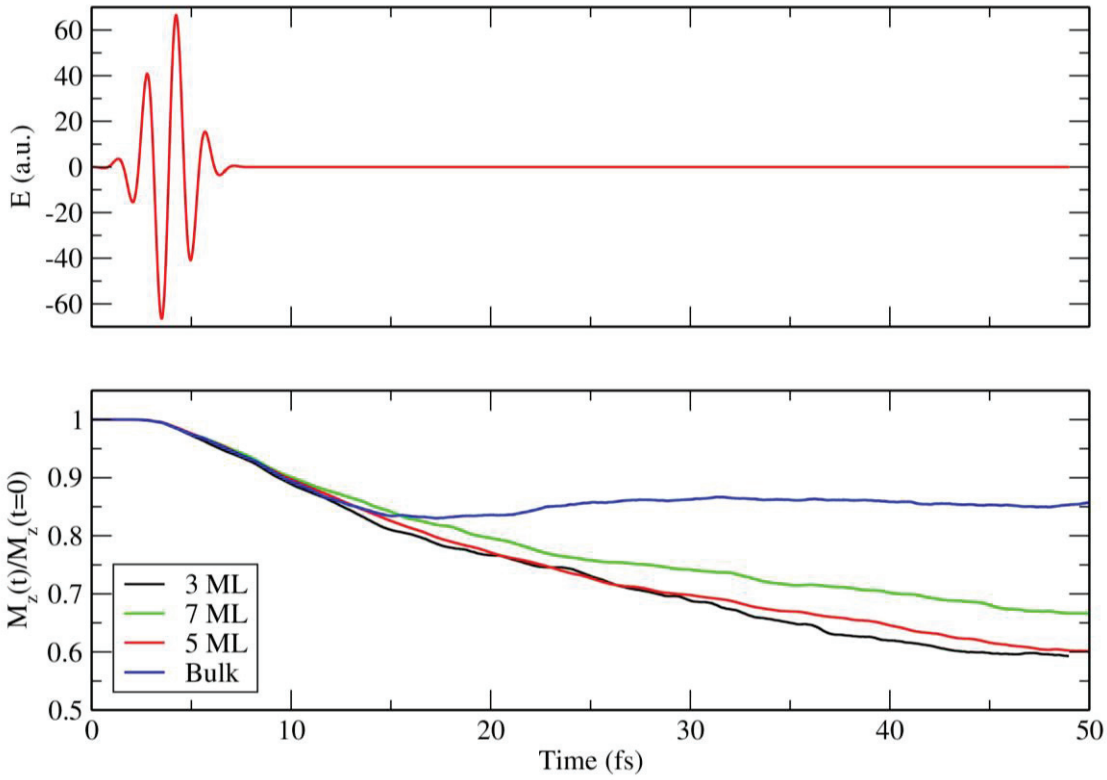

FIGURE 1: Top panel: The electric field of the applied laser pulse with an intensity of 9.3×10^{15} W/cm^2 and a FWHM of 103.35 fs. Lower panel: The dynamics of the *z*-component of the magnetic moment for different layers of Nickel and bulk Nickel simulations.

Conclusions

The phenomena of ultrafast demagnetisation can be put to practical use in designing new electronic devices, however, for this it is crucial to know how significantly the behavior of the surface (or interface) differs from the bulk of the material. To measure demagnetisation experimentally, the technique employed is either probing the surface or the interior of the material. This work shows how the percentage of demagnetisation would be very different when probed with surface sensitive techniques, like Kerr effect, as compared to other techniques that probe either the average or interior of the sample.

Calculation Details

All simulations are performed using Elk [17] code, which is a state-of-the-art all-electron code. Nickel in its face-centered structure having a lattice constant of 3.52 Å is simulated. For bulk calculations a grid of 8×8×8 **k**-points and for film 8×8×1 **k**-point grid is used. For time propagation a time step of 0.002fs was used.

REFERENCES

1. E. Beaurepaire, J.C. Merle, A. Daunois & J.Y. Bigot, "Ultrafast spin dynamics in ferromagnetic nickel," Phys. Rev. Lett. **76**, 4250-4253 (1996).
2. U. Bovensiepen, "Femtomagnetism: Magnetism in step with light," Nat. Phys. **5**, 461-463 (2009).
3. J. Hohlfeld, E. Matthias, R. Knorren & K.H. Bennemann, "Nonequilibrium Magnetization Dynamics of Nickel," Phys. Rev. Lettl **78**, 4861-4864 (1997).
4. A. Scholl, L. Baumgarten, R. Jacquemin & W. Eberhardt, "Ultrafast Spin Dynamics of Ferromagnetic Thin Films Observed by fs Spin-Resolved Two-Photon Photoemission,"Phys. Rev. Lett. **79** , 5146-5149 (1997).
5. M. Aeschlimann et. al.. "Ultrafast Spin-Dependent Electron Dynamics in fcc Co.", Phys. Rev. Lett. **79**, 5158-5161 (1997).
6. H. Regensburger, R. Vollmer & J. Kirschner, "Time-resolved magnetization-induced second- harmonic generation from the Ni(110) surface.", Phys. Rev. B **61**, 14716-14722 (2000).
7. C. Karel, M. Battiato, and P. M. Oppeneer. "Is the controversy over femtosecond magneto-optics really solved?", Nat Phys, 7(9): 665–665, Sep 2011.
8. M. Battiato, K. Carva, and P. M. Oppeneer, "Superdiffusive spin transport as a mechanism of ultrafast demagnetization.", Phys. Rev. Lett., 105:027203, Jul 2010.
9. K. Krieger, J.K. Dewhurst, P. Elliott, S. Sharma & E.K.U. Gross, "Laser induced demagnetization at ultrashort time scales: Predictions of TDDFT.", J. Chem. Theory Comput. **11**, 4870 (2015).
10. P. Elliott, K.Krieger, J.K. Dewhurst, S.Sharma & E.K.U.Gross, "Optimal control of laser- induced spin-orbit mediated ultrafast demagnetization.", New Journal of Physics **18**, 013014(2016).
11. K. Krieger, P. Elliott, T. Mueller, N. Singh, J.K. Dewhurt, E.K.U. Gross, and S. Sharma, "Ultrafast demagnetization in bulk versus thin films: an ab initio study.", J. Phys. Condens. Matter **29**, 224001 (2017).
12. Excited states from time-dependent density functional theory, P. Elliott, F. Furche, and K. Burke, in Reviews in Computational Chemistry, eds. K. B. Lipkowitz and T. R. Cundari, (Wiley, Hoboken, NJ, 2009), pp 91-165.
13. *Fundamentals of Time-Dependent Density Functional Theory, (Lecture Notes in Physics 837)*, eds. M.A.L. Marques, N.T. Maitra, F. Nogueira, E.K.U. Gross, and A. Rubio, (Springer-Verlag, Berlin, Heidelberg, 2012).
14. E. Runge & E.K.U. Gross, "Density-functional theory for time-dependent systems.", Phys. Rev. Lett. **52**, 997 (1984).
15. C.A. Ullrich, Book: "Time-Dependent Density-Functional Theory Concepts and Applications" (Oxford University Press, Oxford, New York, 2011).
16. P. Elliott, T. Müller, J.K. Dewhurst, S. Sharma & E.K.U. Gross, "Ultrafast laser induced local magnetization dynamics in Heusler compounds.", Scientific Reports 6, Article number: 38911(2016)
17. J.K. Dewhurst, S. Sharma & et. al elk.sourceforge.net